The Plastidic Pentose Phosphate Translocator Represents a Link between the Cytosolic and the Plastidic Pentose Phosphate Pathways in Plants[1]

Michael Eicks, Verónica Maurino, Silke Knappe, Ulf-Ingo Flügge, and Karsten Fischer*

Botanisches Institut der Universität zu Köln, Lehrstuhl II, Gyrhofstrasse 15, D–50931 Cologne, Germany

Plastids are the site of the reductive and the oxidative pentose phosphate pathways, which both generate pentose phosphates as intermediates. A plastidic transporter from Arabidopsis has been identified that is able to transport, in exchange with inorganic phosphate or triose phosphates, xylulose 5-phosphate (Xul-5-P) and, to a lesser extent, also ribulose 5-phosphate, but does not accept ribose 5-phosphate or hexose phosphates as substrates. Under physiological conditions, Xul-5-P would be the preferred substrate. Therefore, the translocator was named Xul-5-P/phosphate translocator (XPT). The XPT shares only approximately 35% to 40% sequence identity with members of both the triose phosphate translocator and the phospho*enol*pyruvate/phosphate translocator classes, but a higher identity of approximately 50% to glucose 6-phosphate/phosphate translocators. Therefore, it represents a fourth group of plastidic phosphate translocators. Database analysis revealed that plant cells contain, in addition to enzymes of the oxidative branch of the oxidative pentose phosphate pathway, ribose 5-phosphate isomerase and ribulose 5-phosphate epimerase in both the cytosol and the plastids, whereas the transketolase and transaldolase converting the produced pentose phosphates to triose phosphates and hexose phosphates are probably solely confined to plastids. It is assumed that the XPT function is to provide the plastidic pentose phosphate pathways with cytosolic carbon skeletons in the form of Xul-5-P, especially under conditions of a high demand for intermediates of the cycles.

Plastids are classified as either autotrophic chloroplasts or nongreen plastids (e.g. amyloplasts, leucoplasts, or chromoplasts) according to morphological and biochemical differences. They perform many specialized functions such as photosynthesis, nitrogen assimilation, the synthesis of amino acids and fatty acids, or the storage of carbohydrates and lipids (Bowsher et al., 1992; Emes and Tobin, 1993). These pathways require an extensive exchange of metabolites between plastids and the surrounding cytosol. The exchange processes are mediated by multiple transporters of the inner envelope membrane (Emes and Neuhaus, 1997; Flügge, 1999). Only a small number of transporters have been characterized at the molecular level. These include a dicarboxylate translocator that is involved in ammonia assimilation (Weber et al., 1995); a hexose transporter that exports hexoses, the product of hydrolytic starch degradation, from the plastids (Weber et al., 2000); an ADP/ATP transporter that supplies plastids with energy for biosynthesis of starch, fatty acids, and other compounds (Neuhaus et al., 1997); and phosphate translocator (PT) proteins, which all function as antiport systems using inorganic phosphate or phosphorylated C3 and C6 compounds as counter-substrates.

The PT proteins can be classified into three different groups. The physiological function of the triose phosphate/PT (TPT) is to facilitate the export of fixed carbon from the chloroplast in the form of triose phosphates and represents the daytime path of carbon export during ongoing photosynthesis (Fliege et al., 1978; Flügge et al., 1989; Fischer et al., 1994). The phospho*enol*pyruvate (PEP)/PT (PPT) belongs to the second group of plastidic PTs and mediates the transport into plastids of PEP, which is used as a substrate for the formation of aromatic amino acids via the shikimic acid pathway leading to a series of secondary compounds. A mutant deficient in the PPT gene shows a severe phenotype and is unable to produce anthocyanins as a product of secondary plant metabolism (Fischer et al., 1997; Streatfield et al., 1999). The Glc-6-P/PT (GPT) represents the third PT group transporting Glc-6-P, triose phosphates, and phosphate, whereas other hexose phosphates such as Glc-1-P and Fru-6-P are not transported (Kammerer et al., 1998). Glc-6-P, which has been imported into nongreen plastids is used either for the syntheses of starch and fatty acids or is fed into the plastidic oxidative pentose phosphate pathway (OPPP; Borchert et al., 1989; Bowsher et al., 1992; Emes and Neuhaus, 1997).

The OPPP consists of two branches. The oxidative branch produces ribulose 5-phosphate (Ru-5-P) and reducing power (NADPH) that can be used, for example, for the synthesis of amino acids and fatty acids. In the reversible, nonoxidative branch of the OPPP, Ru-5-P is converted to Rib-5-P by Rib-5-P isomerase (RPI) and to xylulose 5-phosphate (Xul-5-P) by Ru-5-P epimerase (RPEase). Rib-5-P serves as a substrate for nucleotide biosynthesis. Further reactions of the nonoxidative branch lead to interconversion of C7, C6, C5, C4, and C3 sugar phosphates, which are also intermediates of the reductive pentose phosphate cycle. The sugar phosphates generated can be used for other biosynthetic pathways. For example, erythrose 4-phosphate (Ery-4-P) is a substrate for the biosynthesis of aromatic amino acids produced via the shikimic acid pathway. In contrast to animal and yeast cells, the enzymes of the oxidative part of the OPPP are commonly found in both the cytosol and stroma of plant cells (Heber et al., 1967; Schnarrenberger et al., 1973; Emes and Fowler, 1979; Stitt and ap Rees, 1979; Fickenscher and Scheibe, 1986; Graeve et al., 1994; von Schaewen et al., 1995). However, the enzymes of the nonoxidative part of the OPPP have been found predominantly in plastids (Heber et al., 1967; Feierabend and Gringel, 1983; Schnarrenberger et al., 1995; Debnam and Emes, 1999; Henkes et al., 2001). With these findings, the question arises as to the likely fate of cytosolic pentose phosphates produced by the oxidative part of the OPPP. To be further used by the nonoxidative part of the OPPP, transport of pentose phosphates across the plastidic envelope would be required. Earlier reports have indicated that pentose phosphates can be transported both into chloroplasts (Bassham et al., 1968; Lilley et al., 1977) and nongreen plastids (Hartwell et al., 1996; Debnam and Emes, 1999). In nongreen plastids, they support nitrite reduction, indicating that pentose phosphates are recycled through the OPPP to regenerate Glc-6-P that is then reduced to Ru-5-P with the concomitant production of NADPH.

Direct measurements of the permeability of the inner envelope membrane revealed that Rib-5-P is not taken up by spinach (*Spinacia oleracea*) chloroplasts, whereas Ery-4-P is relatively well transported (Heldt, 1976; Fliege et al., 1978). However, because of the low transport rates and because it was assumed that the transport of these sugar phosphates is mediated by the TPT, the only known PT at that time, no further attention has been paid to the molecular characterization and physiological function of this transport process.

In this study, we describe the molecular cloning and characterization of a plastidic pentose PT from Arabidopsis that transports the C5 ketose sugars Xul-5-P and, to a lesser extent, Ru-5-P, but not the aldose Rib-5-P nor hexoses like Glc-6-P. Thus, the Xul-5-P/PT (XPT) represents a fourth class of PTs.

RESULTS

Cloning and Sequence Analysis of the XPT Gene

The Arabidopsis expressed sequence tag (EST) clone 121I21T7 (accession no. T43612) was identified through a database search by its high homology to GPTs from pea (*Pisum sativum*), Arabidopsis, and maize (*Zea mays*; Kammerer et al., 1998). The full-length cDNA was isolated by screening an Arabidopsis cDNA library constructed in the Uni-ZAP XR vector. Sequence analysis of this clone indicated an open reading frame encoding a protein with 417 amino acid residues with a molecular mass of 45 kD. Hydrophobicity distribution analysis of the amino acid sequence suggests that this protein contains about six to eight transmembrane-spanning domains, as is the case for TPT, PPT, and GPT proteins. The hydrophilic amino-terminal part of the protein, approximately 100 amino acid residues in length, comprises the N terminus of the mature protein and the transit peptide that directs the XPT protein to the plastid envelopes and that is proteolytically removed during or after integration into the membrane (Fig. 1). The precise location of the processing site of the XPT is not known but is assumed to be located between amino acid residues 75 and 85 by comparison of the XPT sequence with sequences of other known PT proteins.

Comparison of the amino acid sequence of the XPT coding for the mature part of the protein with all other PTs revealed a low but significant homology to TPTs and PPTs (35%–40% identity), but a higher degree of identity with GPT proteins (about 50% identity). However, the number of identical amino acids between the XPT and GPTs from Arabidopsis was lower than that between the GPTs from different plants that share 79% to 83% identical residues with each other. Thus, the XPT seems to represent a different, fourth group of PTs. This conclusion was confirmed by constructing a phylogenetic tree using the distance matrix method (Saitou and Nei, 1987). As shown in Figure 2, members of the three previously characterized groups of PTs cluster at approximately equal distances from each other, whereas the XPT genes cluster together with the GPT group but branch off earlier. More detailed examination of the sequence corroborates this conclusion (Fig. 1). The TPTs, PPTs, and GPTs, despite their low overall similarities, possess five regions of remarkable similarity (Kammerer et al., 1998) that are also found in the XPT sequence. Moreover, the dipeptide Lys-Arg (amino acid residues 278 and 279 in ZmGPT) that is located in the fourth region of high similarity comprising most of the fifth membrane-spanning region is conserved in all four classes of PTs including the XPT. This dipeptide is very likely involved in binding of the substrate (Flügge and Heldt, 1977, 1979; Fischer et al., 1994). The two amino acid residues located directly upstream and downstream of the Lys-Arg

Transit peptide

```
-70  MIPSVRLSPG PAAFS----- ---GSSLRSK LPSIPS--IS SLKPSKYVVS SLKPLYLAPL DGP--RTAEL K------SRR QPL-----EF RCS    ZmGPT
-85  ..S.L.QPSI SISGSDV-VL RKRHAT.IQL R.QSF.PFS. RE.SQRS... TK...H..C. GVG--NPFGSV .NFESEA.FG .SD-----LV K.G    PsGPT
-66  .VL..KQTLS .KIG----LF RRNP..SLGR S.VSL.-FP. TEL.KRT.LA VS...H.S-- -------SS. R--------A KSP-----VV ..E    AtGPT1
-70  .LS.IKP.SS SFSTAISGSV RRSIPTKLKF S.LLIIKNCH NQSFNAN... HQ...HISSA SN-------- ------FK. --------.V KVE    AtGPT2
-82  ..SLNL-..S LNPG------ -LLHKTRTCQ Q.TRL.---A L.VTNPKPFN HRH..G.S.I PNLQI.DVSA .PLLSLTNPE SSSGFSRKPR SIA    AtXPT
```

Mature protein

```
                                           _____I_____                 _____II_____
ZmGPT  ASAAD----- DKESKTQVVP V-QSEGAQRL KISIYFATWW ALNVIFNIYNKKVLNAFPYP WLTSTLSLAC GSAMMLFSWA TRLVEAPKTD LDFWKVLFPV AVAHTIGHVA  104
PsGPT  .YE..----- --R.EVEGGD GTP..A.KKV .......... ....V.........Y... .........L...I... ..IA.....E...T.... ..........  103
AtGPT1 .YE..--RSE PHPIGDAAAAETK..A.KK. .......... ....V.........Y... .........A ..L...I... ..I..T.... FD...T....  ..........  109
AtGPT2 .YE..--RSR PLDINIELPD E--..--..K. ..G....... ....V.......... ..........L...V... ..IAD.....E...T.... ..........  105
AtXPT  .VGSS--DSN PD.KSDLGEA EKKEKKAKT. QLGIV.GL.Y FQ.IV..F...A..V.... ..LASFQ.FA ..IW..VL.S FK.YPC..IS KP.IIA.LGP .LF.....IS  108

             _____III_____                            _____IV_____
ZmGPT  ATVSMSKVAV SFTHIIKSAE PAFSVLVSRF FLGETFPIPV YLSLLPIIGG CALAAVTELN FNMVGFMGAM ISNLAFVFRN IFSKRGM-KGKSVSGMNYYACLS IMSLVILTPF  216
PsGPT  .......... ........G. .......... I......V.. ......... ...I...... ...I...... .......... ........-............ ...L..A....  215
AtGPT1 .......... ........G. .......... I......TS. ....I..... ...S...... ...I...... .......... .......-.............. ...ML..L....  221
AtGPT2 .......... ........G. .......... .M....L... ......... ...I....I .....IT.... ......K... .......K.-.............. ...M........  217
AtXPT  .C..F..... ....V..... .V...IF.S- L..DSY.LA. W..I...VM. .S......VS ...LG.LS... ...VG..L.. .Y...SLQSF.EID.L.L.G.I. .L..LY.F.V  220

             ____
ZmGPT  AIAMEGPQMW AAGWQKALAE VGP-NVVW-WIAAQSVFYHLY NQVSYMSLDQ ISPLTFSIGN TMKRISVIVS SIIIFHTPVR AVNALGAAIA ILGTFLYS-- ---------Q AKA  317
PsGPT  .......A.. .....T..S. I..-Q..-.V....I..... .........E .......... .......... .........IQ P......... VF......-- ---------. ..Q  316
AtGPT1 ...V...... VD...T...T ...-Q...-.VV...... .......... .......... .......... .....R...Q P......... ........-- ---------. ..L  322
AtGPT2 S..V...... .....N.VSQ ...-F..-.VV...... .......... .......... .......A ....IQ P......... .F......-- ---------. ..Q  318
AtXPT  ..FV..SH-. VP.YH..I.S ..TPSTFYF.VLLSG...... ...S..QA..E .......V.. ....VV...I. TVLV.RN... PL....S... .C......QATAKKKKIEVGGDKKN  335
```

Figure 1. Alignment of XPT and GPT amino acid sequences. The XPT sequence from Arabidopsis (AtXPT) was aligned with GPT sequences from maize (ZmGPT, accession no. AF020813), pea (PsGPT, accession no. AF020814), and two GPTs from Arabidopsis (AtGPT1, accession no. At5g54800; AtGPT2, accession no. At1g61800). Identities of the amino acids between the translocators are indicated by dots. Amino acids are numbered beginning with the first amino acid of the mature proteins. Dashes indicate gaps introduced to maximize alignment. The locations of putative six membrane spanning regions are indicated (I–VI).

motif are characteristic of each PT class. In the case of the GPT, the upstream residues are Thr-Met, a dipeptide that is found in the XPT sequence also, whereas the TPTs and PPTs possess the dipeptide Val-Leu and Cys-Val, respectively (Kammerer et al., 1998). In contrast, downstream of the Lys-Arg motif, the GPT sequences contain the dipeptide Ile-Ser, whereas the XPT protein possesses the dipeptide Val-Val at that position like the PPTs (Fig. 1, bold letters). The TPT proteins are characterized by the amino acid residues Val-Phe at that position. Furthermore, the next dipeptide downstream, Val-Ile, is again conserved in all classes of PTs, whereas the following GPT- (and PPT-) specific Val is changed to Ile in the XPT protein (Fig. 1, bold letters). Whether the latter plays a role in substrate recognition and/or binding has to be elucidated further.

To isolate the XPT gene, an Arabidopsis genomic library was screened by in situ plaque hybridization using the full-length XPT cDNA as a hybridization probe. A 5.0-kb insert of one positive clone was excised, subcloned into the Bluescript vector, and sequenced. The sequence comprised the 5'-non-coding region, 1,912 bp in length; a coding region of 1,254 bp; and the 3'-non-coding region consisting of 1,791 bp (accession no. AF209211). A comparison of the cDNA and genomic sequences indicates that the XPT gene contains no introns. This result was also confirmed by intron-differential reverse transcriptase (RT)-PCR (data not shown). Digestion of genomic DNA with a set of restriction enzymes and subsequent hybridization with the coding region as a probe showed the presence of a single gene in the Arabidopsis genome. In addition, we could identify only one XPT gene in the recently published genome sequence of Arabidopsis (Arabidopsis Genome Initiative, 2000). The XPT gene is located on chromo-

some 5 between the markers g5962 (33.3 cM) and g4568 (33.4 cM). The XPT promoter region was analyzed to localize the basal promoter elements. Two putative TATA box motifs were found to be localized at positions −175 and −189. Also, two putative CAAT box regions at positions −203 and −241 could be detected. Other elements responsible for the interaction with known transcription factors were not evident. It may be noted that the XPT ATG region responsible for the binding of the ribosomal 40S subunit perfectly matches the plant consensus sequence TAAACAATG.

Expression Pattern of the XPT Gene in Arabidopsis

To determine the tissue-specific expression of the XPT gene, an RT-PCR assay was used. An RT-PCR product of 586 bp was amplified to about the same level from RNAs from all tissues examined (flowers, leaves, shoots, and roots; Fig. 3). This is in contrast to the expression profile of the TPT gene, which can be detected only in photosynthetically active tissues as is the case for the LHCP gene. To obtain more specific information on the expression of the XPT gene, e.g. during development, the XPT promoter region (1,276 bp) and 431 bp of the XPT coding sequence were used to generate a translational fusion with the *Escherichia coli* β-glucuronidase (GUS) reporter gene. This construct was stably transferred to Arabidopsis plants via *Agrobacterium tumefaciens*-mediated transformation. Nine transgenic lines were tested for GUS expression patterns (Jefferson et al., 1987). All lines showed similar GUS histochemical staining; differences were observed only in the intensity of GUS staining. GUS expression was observed in vegetative parts, such as leaves of all developmental stages and roots, particularly root tips (Fig. 4A). Trichoms of
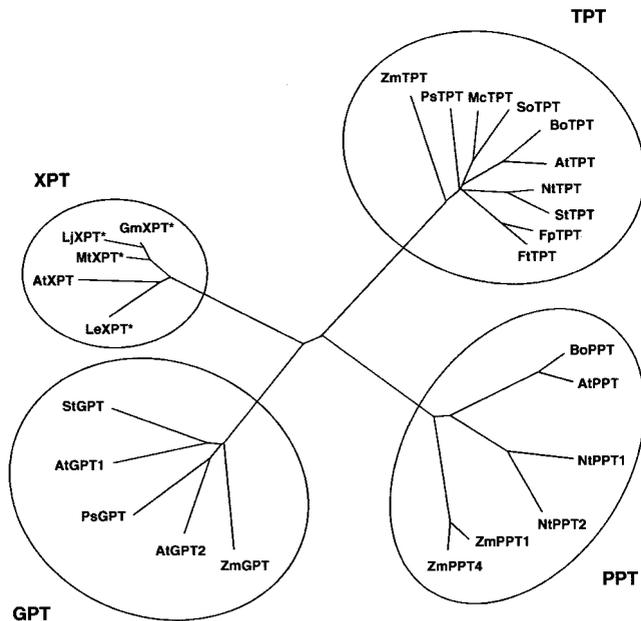
Figure 2. Phylogenetic tree of PT genes using the Maximum Likelihood of the Phylogenetic Analysis Program Package. The tree was constructed on the basis of some of the available TPT, PPT, GPT, and XPT amino acid sequences. The alignment of the sequences was created using the CLUSTAL X program and used for constructing a phylogenetic tree (Higgins et al., 1992). From this treefile, an unrooted tree was drawn using the Drawtree program from the PHYLIP 3.572 program package. At, Arabidopsis; Bo, *Brassica oleraceum*; Fp, *Flaveria pringlei*; Ft, *Flaveria trinervia*; Gm, soybean (*Glycine max*); Le, *Lycopersicon esculentum*; Lj, *Lotus japonicus*; Mc, *Mesembryanthemum crystallinum*; Mt, *Medicago truncatula*; Nt, tobacco (*Nicotiana tabacum*); Ps, pea; St, *Solanum tuberosum*; Zm, maize. Asterisks indicate EST sequences.

leaves and stems were highly stained and stems also became stained after cross section of the tissue (Fig. 4B). In the floral tissue, GUS activity is restricted to sepals, filaments, the upper part of the style, and the stigma, but no activity was observed in petals, young ovaries, and the anthers (Fig. 4C). Moreover, strong GUS activity was obtained in the pods and seeds of developed fruits, but no staining was evident during the early fruit development period (not shown).

Transport Characteristics of the XPT Protein

Heterologous expression of cDNAs in yeast, protein purification by affinity chromatography, and reconstitution of transport activity in liposomes are current methods to characterize the function of translocator proteins (Kasahara and Hinkle, 1977; Flügge, 1998; Hanke et al., 1999). In recent years, several members of the three groups of known plastidic PTs have been functionally characterized using these techniques (Loddenkötter et al., 1993; Fischer et al., 1997; Kammerer et al., 1998). To elucidate the substrate specificity of the XPT protein, the Arabidopsis XPT cDNA coding for amino acid residues −8 to 335 (see Fig. 1) was extended by an N-terminal His-6 tag

and subsequently cloned into the yeast expression vector SAP-E. As outlined above, the exact position of the processing site is not known. However, this appears to be of minor importance because previous experiments had shown that the expression of even a whole precursor protein in yeast leads to the production of a functional transporter with transport characteristics almost identical to the authentic protein (Weber et al., 1995). The XPT construct was then used to transform cells of fission yeast (*Schizosaccharomyces pombe*). The XPT protein subsequently was isolated to near homogeneity from the membrane fraction by Ni^{2+}-nitrilotriacetic acid agarose chromatography (data not shown) and reconstituted into liposomes. Table I shows the substrate specificities of the XPT protein reconstituted into liposomes that had been preloaded with different phosphorylated metabolites as exchangeable counter-substrates. For comparison, the substrate specificity of the His-6-tagged GPT from pea roots (Kammerer et al., 1998) is shown. Inorganic phosphate, triose phosphates, 3-P-glycerate, and Xul-5-P evidently are all equally well accepted as counter-substrates by the XPT. Transport of phosphate was also supported by liposomes preloaded with Ery-4-P and Ru-5-P, albeit to a lesser extent, whereas the data demonstrate that Rib-5-P is not accepted as a counter-substrate. PEP and Glc-6-P are only poorly transported. This is quite surprising considering the relatively close relationship of XPT and the GPTs. Moreover, XPT does not transport other hexose phosphates like Glc-1-P or Fru-6-P. We also tested if the GPT is capable of transporting pen-
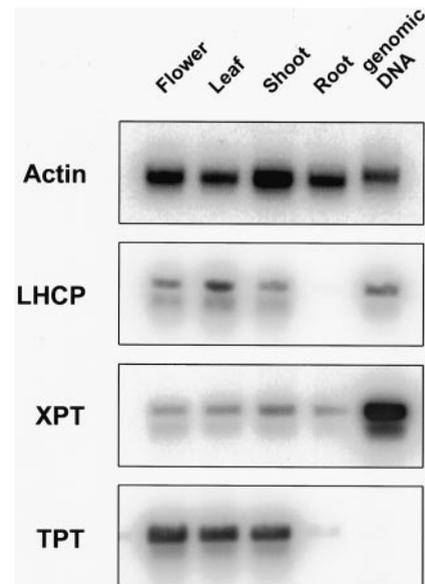
Figure 3. Analysis of *XPT* transcript levels by quantitative RT-PCR. RNAs from flowers, leaves, shoots, and roots were analyzed. *XPT* transcripts are present in all organs, whereas expression of the *TPT* gene is restricted to photosynthetically active tissues. Actin was used as a loading control, LHCP as a root-negative control. RNAs and genomic DNA were prepared from Arabidopsis Col-0.
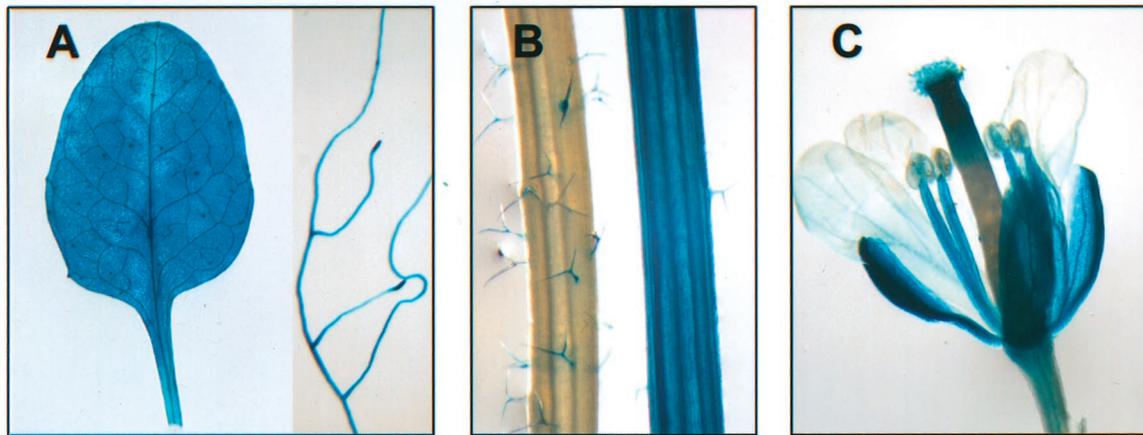
Figure 4. Histochemical localization of GUS activity from the XPT promoter-*GUS* reporter in Arabidopsis. A, Fully developed rosette leaf with equal staining in the mesophyll and vascular tissue (left) and GUS staining of roots (right). B, Stem with trichoms before (left) and after (right) cross section. C, Flower with already elongated ovary, with GUS staining in sepals, filaments, the upper part of the style, and the stigma.

tose phosphates. As shown in Table I, the ketoses Xul-5-P and Ru-5-P are transported quite well and with efficiencies about twice as high as the C_4 sugar Ery-4-P. It is remarkable, and in contrast to the XPT, that the aldose Rib-5-P can also serve as a counter-substrate for the GPT.

Table I. *Determination of substrate specificities of recombinant phosphate translocator proteins expressed in yeast cells*

Internal Liposomal Substrate[a]	Purified Recombinant (His-6-Tagged) Translocator Protein from Fission Yeast Cells[b]	
	XPT (Arabidopsis)	GPT (pea root plastids)[c]
Phosphate	=100	=100
Triose phosphates	88 ± 12	112 ± 5
3-Phosphoglycerate	69 ± 10	50 ± 1
PEP	10 ± 1	20 ± 1
Ery-4-P	34 ± 5	28 ± 8[d]
Rib 5-P	2 ± 1	29 ± 0[d]
Ru-5-P	28 ± 4	53 ± 6[d]
Xul-5-P	81 ± 8	54 ± 12[d]
Glc 6-P	6 ± 2	90 ± 9
Glc 1-P	<1	<1
ADP-Glc	<1	ND[e]
Fru 6-P	<1	<1
6-Phosphogluconate	<1	ND
Pyrophosphate	<1	ND

[a] The liposomes had been preloaded with 30 mM substrate as indicated. [b] Purification and transport measurement were performed as described in "Materials and Methods." Transport of [^{32}P]-phosphate is given as a percentage of the activity measured for proteoliposomes preloaded with inorganic phosphate (minus values obtained for liposomes that were pre-inhibited). The 100% exchange activities (micromoles per milligram of protein per minute) of the recombinant proteins were 1.4 (XPT) and 1.2 (GPT). Mean values are from three to five different experiments ± SE. [c] Data from Kammerer et al. (1998) except those indicated by footnote d. [d] Data from two to three independent experiments ± SE. [e] ND, Not determined.

Table II shows apparent kinetic constants of the XPT. The K_m(app)(phosphate) was determined to be about 1.0 mM and thus is comparable to values obtained for the TPT, PPT, and GPT proteins (Fischer et al., 1997; Kammerer et al., 1998). The low K_i values for triose phosphates (0.4 mM) and Xul-5-P (0.8 mM) indicate that these compounds most effectively compete with phosphate for binding to the XPT. Glc-6-P and Rib-5-P both have very high K_i values (66 and 22 mM, respectively), reflecting their poor transport rates. In the case of 3-P-glycerate, a significant transport rate is opposed by a high K_i value (10.6 mM), whereas PEP is rather well bound to the protein (K_i value, 2.1 mM) but only poorly transported. The intermediate K_i values for Ery-4-P and Ru-5-P (3.3 and 3.5 mM, respectively) reflect their intermediate transport rates. Taken together, it is evident that Rib-5-P and Glc-6-P are not transported at all by the XPT. In vivo, the transport of PEP, 3-P-glycerate, Ery-4-P,

Table II. *Apparent (app) K_m (phosphate) and K_i values of the recombinant XPT for various phosphorylated metabolites*

Substrate	Kinetic Constants for the Transport of [^{32}P]Phosphate[a] (K_m (app) (mM): 1.0 ± 0.2)
	K_i (app) (mM)
Triose phosphates	0.4 ± 0.1
3-Phosphoglycerate	10.6 ± 2.9
PEP	2.1 ± 0.2
Ery-4-P	3.3 ± 0.5
Rib-5-P	22 ± 1
Ru-5-P	3.5 ± 0.3
Xul-5-P	0.8 ± 0.1
Glc-6-P	66 ± 7

[a] The transport activities were measured as described in "Materials and Methods" and in the legend to Table I. All experiments were performed using liposomes that had been preloaded with 30 mM inorganic phosphate. Mean values are from three different experiments ± SE.

and Ru-5-P is unlikely when the rather high concentrations necessary to achieve this are taken into account. Thus, the XPT represents a plastidic PT preferentially transporting phosphate, triose phosphates, and Xul-5-P, but not Glc-6-P or other hexose phosphates. This is in contrast to the transport characteristics of the GPT (Table II), which transports Glc-6-P, triose phosphates, and 3-P-glycerate, but also pentose phosphates at rates similar to that of 3-P-glycerate.

Database Search

As outlined above, Ru-5-P is one product of the oxidative part of the OPPP and can be converted to Rib-5-P by RPI and to Xul-5-P by RPEase. Both pentose phosphates subsequently are converted into triose phosphates and hexose phosphates by the two other enzymes of the OPPP, namely transketolase and transaldolase. It is still a matter of debate if the enzymes of the nonoxidative branch of the OPPP are present both in the plastids and the cytosol or are restricted only to plastids. Therefore, we performed a sequence homology search of the GenBank database to identify putative genes in the Arabidopsis genome coding for RPI, RPEase, and also for transketolases and transaldolases. This strategy is based on the findings that all known and characterized stromal proteins, e.g. the enzymes of the Calvin Cycle or the shikimate pathway, possess N-terminal extensions that direct these proteins to the stroma. Therefore, the presence of transit peptides can be used to distinguish between cytosolic and plastidic isoforms.

One gene probably coding for a plastidic isoform of RPEase (accession no. AAD09954) and three genes encoding potential cytosolic isoforms (accession nos. AAK43856 and AAF03437, both on chromosome 3, and AAG52146 on chromosome 1) could be identified. The first two cytosolic isoforms differ only in one insertion, which might be an artifact due to a misestimated intron-exon structure. Moreover, we found a large number of ESTs from multiple higher plants. Most if not all plants apparently possess cytosolic RPEases.

The Arabidopsis genome contains three different genes encoding RPI that are located on chromosomes 1, 2, and 3 (accession nos. AAK26040, AAD14529, and AAG51427). One of the enzymes probably represents a plastidic isoform because it shows a high homology to the plastidic RPI from spinach (Martin et al., 1996) and, in addition, a plastidic presequence is found at the N terminus (accession no. AAG51427, chromosome 3). The two other RPIs presumably represent cytosolic isoforms because they lack any obvious N-terminal plastid-targeting sequence. Although the cytosolic localization of these enzymes has yet to be established experimentally, it can be assumed that Ru-5-P can be converted to Rib-5-P and Xul-5-P in both the plastids and the cytosol.

Two highly homologous genes coding for plastidic isoforms of transketolases could be identified in the

Arabidopsis genome (accession nos. AAB82634 and T47886 on chromosomes 2 and 3, respectively). However, no cytosolic isoforms were identified. Both Arabidopsis transketolases share high homology with the plastidic transketolase from spinach (Flechner et al., 1996). No other genes or ESTs were found in the databases encoding cytosolic isoenzymes except for the desiccation-tolerant resurrection plant *Craterostigma plantagineum*. This plant possesses two cytosolic transketolase isoenzymes in addition to a plastidic isoform (Bernacchia et al., 1995). These cytosolic isoforms might play a role in the particular octulose metabolism that is connected to the desiccation-tolerant physiology of this plant.

Similar to the transketolases, the database only reveals two different transaldolase genes in the Arabidopsis genome (accession nos. AAG12571 and CAB87149 on chromosomes 1 and 5, respectively), coding for proteins, 405 and 576 amino acid residues in length, respectively. They only share 67 identical amino acid residues but both possess plastidic presequences; cytosolic isoforms seem to be absent. Taken together, it seems likely that the cytosolic OPPP in Arabidopsis can proceed to the stage of interconvertible pentose phosphates (Ru-5-P, Rib-5-P, and Xul-5-P), but not further.

DISCUSSION

In this study, we describe the molecular and functional characterization of a plastidic pentose PT from Arabidopsis that exhibits a particularly high homology to GPT proteins from various plants. The transporter was heterologously expressed in yeast cells and the transport characteristics of the purified protein revealed that it accepts mainly inorganic phosphate, triose phosphates, and Xul-5-P as substrates and, to a lesser extent, Ru-5-P and Ery-4-P; Rib-5-P is not transported. Ru-5-P and Ery-4-P are, however, only poorly bound to the transporter and will presumably not be transported under physiological conditions (Tables I and II). Therefore, this new plastidic transporter was named Xul-5-P/PT (XPT).

It is remarkable that Glc-6-P, the preferred substrate of the GPT proteins, is not transported by the XPT. On the other hand, it turned out that the GPT was also able to mediate the transport of pentose phosphates and Ery-4-P (Table I). Thus, Arabidopsis contains two different translocators that are, in principle, capable of transporting pentose phosphates. However, in vivo transport of pentose phosphates by the GPT appears unlikely because these substrates have to compete with concentrations of Glc-6-P as high as 1 mM in the stroma and up to 6 mM in the cytosol (Stitt et al., 1980; Gerhardt et al., 1987; Winter et al., 1994). In addition, the stroma and the cytosol contain millimolar concentrations of triose phosphates, 3-P-glycerate, and inorganic phosphate, which are also GPT substrates. In contrast, the con-

centration of total pentose phosphates in the stroma is approximately 0.1 mM (Flügge et al., 1980, 1982; Heldt et al., 1980), i.e. the concentration of each pentose phosphate is below 0.1 mM. It is unfortunate that to our knowledge, the actual concentration of pentose phosphates in the cytosol of plant cells is not known, but it is reasonable to assume that their concentration is not far above the stromal level. It can be assumed that, under physiological conditions, the transport of pentose phosphates (i.e. Xul-5-P) is mediated solely by the XPT. Transport of Xul-5-P by the XPT cannot be competed by Glc-6-P, which is a substrate of the GPT, but not of the XPT.

The XPT was shown to transport pentose phosphates except for Rib-5-P. This is in contrast to observations that isolated plastids from pea roots seem to import both Rib-5-P and Ru-5-P (Hartwell et al., 1996; Debnam and Emes, 1999). The reason for this discrepancy is not clear. One possibility could be that pea root plastids possess a pentose PT with different substrate specificities or, more likely, that Rib-5-P is transported by the GPT. On the other hand, plastid preparations could be contaminated by stromal enzymes released from broken plastids. This would result in the conversion of Rib-5-P and Ru-5-P to Xul-5-P, which is then imported into the isolated plastids.

A phylogenetic analysis showed that the Arabidopsis XPT and XPT-like sequences from other plants cluster apart from the GPT protein sequences (Fig. 2). The XPT proteins contain, besides a remarkably high degree of similarity to the GPTs, several amino acid exchanges, some of them residing in well-conserved parts of the GPT sequences (Fig. 1). Whereas the GPT gene is expressed predominantly in nongreen tissues that are involved in the storage of photoassimilates (Kammerer et al., 1998), the XPT gene is more regularly expressed in plant tissues (Figs. 3 and 4), indicating a more general role of the XPT in plant metabolism. The reason why the XPT gene is obviously absent in the male reproductive organs (and in petals) remains to be elucidated.

In an attempt to identify all genes in the Arabidopsis genome encoding the four enzymes of the nonoxidative branch of the OPPP, we performed a sequence homology search of the GenBank database. The database search provided convincing evidence that higher plants possess cytosolic isoforms of RPEase and RPI. This observation is corroborated by the recent findings of Kopriva et al. (2000), who isolated cDNAs from rice (*Oryza sativa*), maize, and Arabidopsis encoding cytosolic isoforms of RPEase. The amino acid sequence of the Arabidopsis RPEase showed a higher degree of identity to cytosolic RPEases from yeast and animal cells than to chloroplastic isoforms from plants (Nowitzki et al., 1995). Based on these findings, it can be concluded that plant cells are able to convert Ru-5-P generated in the cytosol to both Rib-5-P and Xul-5-P, the former serving as substrate for nucleotide synthesis, the latter

being substrate for the XPT. In contrast, the two other enzymes of the nonoxidative branch of the OPPP, transketolase and possibly also transaldolase, are probably exclusively confined to the stroma in higher plants, i.e. plant cells are not able to recycle pentose phosphates into triose phosphates and hexose phosphates in the cytosol. However, the apparent absence of genes encoding cytosolic isoforms could also be due to a failure to identify non-homologous transaldolase and transketolase genes. This seems unlikely for two reasons. First, the cytosolic and plastidic isoforms in *C. plantagineum* are encoded by highly homologous genes (Bernacchia et al., 1995). Second, the genomic data are corroborated by biochemical data showing the mostly exclusive localization of transaldolase and transketolase activity in plastids from spinach, maize, and pea. Only in tobacco, Debnam and Emes (1999) showed a significant part of the transaldolase and transketolase to be located in the cytosol, whereas Henkes et al. (2001) could not detect significant cytosolic activities of these enzymes in tobacco plants. However, our conclusions regarding the distribution of OPPP enzymes in Arabidopsis can probably not be generalized to all plant species.

From the data presented here, we conclude that the main physiological function of the XPT is the translocation of Xul-5-P produced in the cytosol into plastids to enable further metabolization of this pentose phosphate. Xul-5-P is an intermediate of both the reductive pentose phosphate cycle (Calvin cycle) and the OPPP. Both cycles provide carbon skeletons for other biosynthetic reactions. For example, Rib-5-P is used for the biosynthesis of nucleotides and Ery-4-P is an immediate precursor of the shikimate pathway leading to a multitude of aromatic compounds (Jensen, 1985; Dennis et al., 1997; Henkes et al., 2001). Under some conditions, more than 20% of fixed carbon in the form of Ery-4-P and PEP, the other precursor of the shikimate pathway imported into the plastids via the PPT (Fischer et al., 1997), is directed to the synthesis of aromatic compounds (Herrmann and Weaver, 1999). It has been shown previously that Ery-4-P cannot be withdrawn from the Calvin cycle in large amounts without depleting the cycle (Geiger and Servaites, 1994). Recent work on tobacco demonstrated that a reduced supply of Ery-4-P, due to an antisense repression of plastidic transketolase activity, results in an inhibition of photosynthesis and a significantly decreased content of aromatic amino acids and soluble phenylpropanoids (Henkes et al., 2001). Also, mutants defective in the PPT show a severe phenotype and strong alterations in secondary metabolism (Streatfield et al., 1999). These data indicate that flux into the plastidic secondary metabolism can be limited by the supply of precursors provided by primary metabolism. Under conditions when significant amounts of intermediates are removed from the pentose phosphate cycles, the XPT could provide the plastids with carbon skeletons in the form of
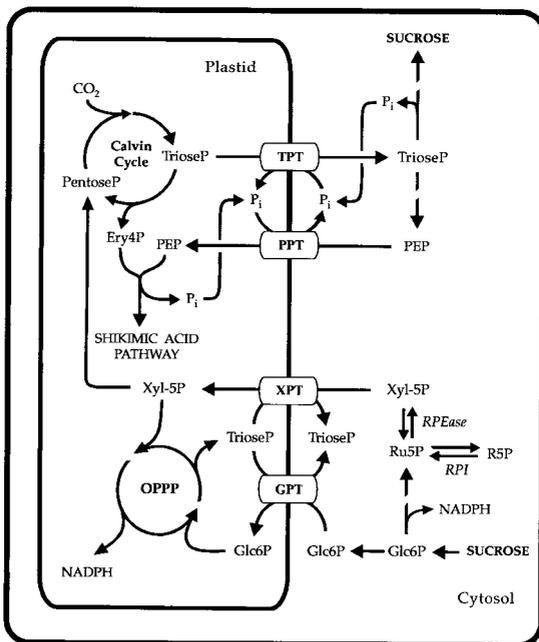
Figure 5. Proposed functions of the four plastidic PT proteins. The TPT mediates the export of carbon from the Calvin cycle in the form of triose phosphates that can be converted to PEP by glycolytic sequences in the cytosol. PEP is imported into the plastids via the PPT to provide the substrate for the shikimic acid pathway. The GPT imports Glc-6-P into the plastids for the syntheses of starch and fatty acids (not shown) and as a substrate for the OPPP yielding triose phosphates. Triose phosphates can serve as a counter-substrate of either the GPT or the XPT. The XPT provides the plastids with Xul-5-P, which is produced in the cytosol from Glc-6-P by the oxidative branch of the OPPP and via RPEase/RPI. Xul-5-P can be used to replenish both the Calvin cycle and the OPPP.

Xul-5-P, generated in the cytosol (Fig. 5). It is suggested that the XPT might play a key role in the cooperation between reactions providing pentose phosphates in the cytosol and the pentose phosphate cycles in the plastids. The analysis of a maize mutant that is deficient in cytosolic 6-phosphogluconate dehydrogenase activity recently demonstrated that cytosolic sequences of the OPPP are necessary to provide reductants for biosynthetic reactions in the plastids under conditions of an increased demand for NADPH (Averill et al., 1998). The mechanism by which such an exchange of reductants between the cytosol and the plastids occur is unclear but might involve the activity of the XPT. Xul-5-P generated by the cytosolic sequences of the OPPP can be transported into the plastids and fed into the OPPP, which produces NADPH.

In yeast, animals, and plants, the OPPP has an additional important function in the response against oxidative stress by delivering electrons for the reduction of active oxygen species like superoxide (O_2^-) and hydrogen peroxide (Izawa et al., 1998). In plants, this process occurs via the ascorbate-glutathione cycle (Noctor and Foyer, 1998). Glc-6-P dehydrogenase and 6-phosphogluconate dehydrogenase (and the en-

zymes of the ascorbate-glutathione cycle) recently were detected in peroxisomes, where they are involved in the scavenging of hydrogen peroxide (Corpas et al., 1998; Corpas et al., 2001). It is tempting to speculate that the XPT is also responsible for the transport of peroxisome-derived pentose phosphates into plastids. Work is in progress to analyze whether the transport of pentose phosphates into plastids, mediated by the XPT, is linked to oxidative stress responses in plant cells.

MATERIALS AND METHODS

Plant Material

Arabidopsis ecotype Columbia was used in all experiments. Seedlings were grown at 20°C under a 12-h-light/12-h-dark regime with approximately 180 μmol photons m^{-2} s^{-1}.

Cloning and Sequencing Procedures

Radiochemicals were purchased from Amersham-Pharmacia (Braunschweig, Germany). Reagents and enzymes for recombinant DNA techniques were obtained from Promega (Heidelberg). Recombinant DNA techniques were performed according to standard procedures (Ausubel et al., 1994).

The Arabidopsis EST 121I21T7 that showed a high homology to the pea (*Pisum sativum*) GPT (Kammerer et al., 1998) was used as probe to screen an Arabidopsis cDNA library constructed in the Uni-ZAP XR vector. The clone containing the longest insert was sequenced completely. The full-length cDNA (XPT) was used as a hybridization probe for a plaque hybridization screening of an Arabidopsis genomic library constructed in EMBL3 SP6/T7 (CLONTECH, Palo Alto, CA). A positive plaque was purified, and an insert of approximately 5.0 kb was excised and subcloned into the vector pBluescript SK$^+$ (Stratagene, La Jolla, CA) for sequencing. Sequencing was performed from both 5' and 3' ends. The plasmid was digested with *Pst*I, *Xho*I, and *Bam*HI and the fragments obtained were subcloned into the vector pBluescript SK$^+$ and sequenced on both strands. In addition, specific oligonuclotide primers were used to complete the sequence. DNA sequences were determined by the dideoxynucleotide chain termination method (ABI PRISM Ready Reaction DyeDeoxyTM Terminator Cycle Sequencing Kit, PerkinElmer Instruments, Rodgau-Jügesheim, Germany).

Southern Analysis

Genomic DNA from the ecotype Columbia was extracted as described by Ausubel et al. (1994). Ten micrograms of DNA was digested with each of six restriction endonucleases at 37°C for 5 h. Restricted DNA was fractionated on a 0.7% (w/v) agarose gel, denatured, and blotted onto a Hybond N$^+$ membrane (Amersham Pharmacia Biotech). Hybridization was performed with the [^{32}P]-labeled full-length cDNA as probe.

Construction of GUS Reporter Vector and Plant Transformation

The GUS gene was cloned downstream of the XPT promoter. The XPT promoter was obtained by cutting the XPT gene (accession no. AF209211) with the restriction enzymes *Sac*I and *Nco*I. The fragment obtained, 1,707 bp in length and comprising 1,276 bp of the promotor region and 431 bp of the coding region, was ligated into the *Hin*dIII site of the plasmid pBluescript SK$^+$ (Stratagene). This construct was digested with *Pst*I, filled in, and subsequently digested with *Xba*I. The resulting 5′-*Xba*I/3′-blunt end fragment was cloned into the *Xba*I-*Sma*I sites of the binary vector pGPTV-BAR carrying the *Escherichia coli* gene *GUS* (Jefferson et al., 1987) to generate a translational fusion of the XPT sequences and the *GUS* gene. This construct was introduced into *Agrobacterium tumefaciens* cells strain GV3101 prior to plant transformation by vacuum infiltration (Bechtold et al., 1993). These plants (ecotype Columbia) were allowed to flower and produce seeds. T$_1$ seedlings were grown as described above and transformants were selected with BASTA, verified by PCR analysis, and analyzed for the distribution of GUS activity (Jefferson et al., 1987).

RT-PCR Analysis

First strand cDNA was synthesized using the SuperScript II RNase H$^-$ RT Kit (Gibco BRL, Karlsruhe, Germany). RNA was prepared according to Ausubel et al. (1994). Primers used for amplification of the XPT cDNA were 5′-CCGTTGGCT CATCGGATTCAA-3′ (XPT forward) and 5′-GCTCTGTAAGCTACGTTTAGA-3′ (XPT reverse; 22 cycles), resulting in a 586-bp amplificate. Primers used for the amplification of actin were 5′-TGTACGCCAGTGGT-CGTACAACC-3′ (forward) and 5′-GGAGCAAGAATGGA-ACCACCG-3′ (reverse; 22 cycles); for LHCP, 5′-TCCATC-AGGCAGCCCATGGTA-3′ (forward) and 5′-CAGTGACG-ATGGCTTGAACGAAG-3′ (reverse; 16 cycles); and for the TPT, 5′-CTGAAGGTGGAGATACCGCTG-3′ (forward) and 5′-GAGTGCGATGATGGAGATGTA-3′ (reverse; 20 cycles). Amplification conditions were as follows: 3 min at 96°C; 16 to 22 cycles of 96°C for 30 s, 50°C for 30 s, and 72°C for 60 s, followed by incubation for 5 min at 72°C. PCR products were separated on a 1.5% (w/v) agarose gel and stained with ethidium bromide.

Heterologous Expression of the XPT in Yeast and Purification of the Recombinant Protein

The DNA encoding the mature part of the translocator (amino acid residues 75–417) was obtained from the complete cDNA (cloned into the vector pBluescript SK$^+$, see above) by digestion with *Xho*I, a subsequent fill in, and a second digestion with *Sal*I. The resulting DNA fragment subsequently was cloned directionally into the blunted *Bam*HI-cut and *Sal*I-digested *E. coli* expression vector pQE32 (QIAGEN, Hilden, Germany), resulting in clone mXPT/pQE. This clone contained a new ATG codon and a His-6 tag fused in frame to the N terminus of the mature part of the XPT protein. This construct was released by

digestion with *Eco*RI and *Sal*I. After the attachment of an additional *Eco*RI site upstream of the His-6-mXPT construct by a further cloning step using the pGEM-T Easy vector (Promega), the DNA fragment was cloned into the yeast expression vector SAP-E (Truernit et al., 1996), resulting in clone mXPT/SAP-E. This vector contains the *Saccharomyces cerevisiae LEU2$^+$* gene as a selectable marker downstream of an ADH promoter-PMA1 terminator box with a unique *Eco*RI cloning site in between. After transformation of the Leu-auxothrophic fission yeast (*Schizosaccharomyces pombe*) strain *1-32*, cells were grown on selective plates and in liquid media. Cells were harvested, disrupted in a buffer containing 10 mM Tris-HCl, pH 7.5, 1 mM EDTA, 300 μg mL^{-1} phenylmethylsulfonylfluoride, and the 100,000g membrane fraction containing the expressed mXPT-His-6 protein was prepared by ultracentrifugation.

Reconstitution of Transport Activities

Reconstitution of the transport activity was performed essentially as described by Flügge (1992) and Fischer et al. (1994), with slight variations. Liposomes were prepared from acetone-washed soybean (*Glycine max*) phospholipids (120–130 mg mL^{-1}) by sonication for 4 to 7 min on ice in 100 mM Tricine-KOH, pH 7.8, 30 mM potassium gluconate, and 30 mM substrate as indicated. Yeast membranes were solubilized using 1.5% to 3% (w/v) n-dodecyl maltoside as detergent and directly reconstituted or subjected to purification via metal affinity chromatography on Ni^{2+}-nitrilotriacetic acid agarose (QIAGEN) before being added to the liposomes (Loddenkötter et al., 1993). Incorporation into the liposomes was achieved by a freeze-thaw step. After sonication, the external medium was removed by passing the liposomes over Sephadex G-25 columns. Eluted proteoliposomes were used for transport, which was initiated by addition of [^{32}P]phosphate (0.25 mM) as the external counterexchange substrate and terminated after 45 to 60 s by the addition of a mixture of pyridoxal 5′-phosphate (58 mM), diisothiocyanostilbene disulfonic acid (3 mM), and mersalyl (10 mM; final concentrations). In control samples, the inhibitors were added prior to the addition of the labeled substrate. External radioactivity was subsequently removed from the reaction mixture by passing the liposomes over a Dowex AG1-X8 anion-exchange column. The radioactivity of the eluate was determined by liquid scintillation counting. In control experiments, the linearity of the transport with time was checked to confirm that initial rates were measured.

LITERATURE CITED

Arabidopsis Genome Initiative (2000) Analysis of the genome sequence of the flowering plant *Arabidopsis thaliana*. Nature **408:** 796–815

Ausubel SF, Brent R, Kingston RE, Moore DD, Seidmann JG, Smith JA, Struhl K (1994) Current Protocols in Molecular Biology. John Wiley and Sons, New York

Averill RH, Bailey-Serres J, Kruger NJ (1998) Co-operation between cytosolic and plastidic oxidative pentose phosphate pathway revealed by 6-phosphogluconate dehydrogenase deficient genotypes of maize. Plant J **14:** 449–457

Bassham JA, Kirk M, Jensen RG (1968) Photosynthesis by isolated chloroplasts: I. Diffusion of labeled photosynthetic intermediates between isolated chloroplasts and suspending medium. Biochim Biophys Acta **153:** 211–218

Bechtold N, Ellis J, Pelletier G (1993) In planta *Agrobacterium*-mediated gene transfer by infiltration of adult *Arabidopsis thaliana* plants. C R Acad Sci Paris Life Sci **316:** 1194–1199

Bernacchia G, Schwall G, Lottspeich F, Salamini, Bartels D (1995) The transketolase gene family of the resurrection plant *Craterostigma plantagineum*: differential expression during the rehydration phase. EMBO J **14:** 610–618

Borchert S, Grosse H, Heldt HW (1989) Specific transport of inorganic phosphate, glucose 6-P, dihydroxyacetone phosphate and 3-phosphoglycerate into amyloplasts from pea roots. FEBS Lett **253:** 183–186

Bowsher CG, Boulton EL, Rose J, Nayagam S, Emes MJ (1992) Reductant for glutamate synthase is generated by the oxidative pentose phosphate pathway in non-photosynthetic root plastids. Plant J **2:** 893–898

Corpas FJ, Barroso JB, del Rio LA (2001) Peroxisomes as a source of reactive oxygen species and nitric oxide signal molecules in plant cells. Trends Plant Sci **6:** 145–150

Corpas FJ, Barroso JB, Sandalio LM, Distefano S, Palma JM, Lupianez JA, del Rio LA (1998) A dehydrogenase-mediated recycling system of NADPH in plant peroxisomes. Biochem J **330:** 770–784

Debnam PM, Emes MJ (1999) Subcellular distribution of enzymes of the oxidative pentose phosphate pathway in root and leaf tissues. J Exp Bot **50:** 1653–1661

Dennis DT, Huang Y, Negm FB (1997) Glycolysis, the pentose phosphate pathway and anaerobic respiration. *In* DT Dennis, DH Turpin, DD Lefebvre, DB Layzell, eds, Plant Metabolism. Longman, London, pp 105–127

Emes MJ, Fowler MW (1979) Intracellular interactions between the pathways of carbohydrate oxidation and assimilation in plant roots. Planta **145:** 287–292

Emes MJ, Neuhaus HE (1997) Metabolism and transport in non-photosynthetic plastids. J Exp Bot **48:** 1995–2005

Emes MJ, Tobin AK (1993) Control of metabolism and development in higher plant plastids. Int Rev Cytol **145:** 149–216

Feierabend J, Gringel G (1983) Plant ketolases: subcellular distribution, search for multiple forms, site of synthesis. Z Pflanzenphysiol **110:** 247–258

Fickenscher K, Scheibe R (1986) Purification and properties of the cytoplasmatic glucose-6-P dehydrogenase from pea leaves. Arch Biochem Biophys **247:** 393–402

Fischer K, Arbinger B, Kammerer B, Busch C, Brink S, Wallmeier H, Sauer N, Eckerskorn C, Flügge UI (1994) Cloning and *in vivo* expression of functional triose phosphate/phosphate translocators from C₃- and C₄-plants: evidence for the putative participation of specific amino acid residues in the recognition of phospho*enol*pyruvate. Plant J **5:** 215–226

Fischer K, Kammerer B, Gutensohn M, Arbinger B, Weber A, Häusler R, Flügge UI (1997) A new class of plastidic phosphate translocators: a putative link between primary and secondary metabolism by phospho*enol*pyruvate/phosphate antiporter. Plant Cell **9:** 453–462

Flechner A, Dressen U, Westhoff P, Henze K, Schnarrenberger, Martin W (1996) Molecular characterization of transketolase active in the Calvin cycle of spinach chloroplasts. Plant Mol Biol **32:** 475–484

Fliege R, Flügge UI, Werdan K, Heldt HW (1978) Specific transport of inorganic phosphate, 3-phosphoglycerate and triosephosphates across the inner membrane of the envelope in spinach chloroplasts. Biochim Biophys Acta **502:** 232–247

Flügge UI (1992) Reaction mechanism and asymmetric orientation of the reconstituted chloroplast phosphate translocator. Biochim Biophys Acta **1110:**112–118

Flügge UI (1998) Metabolite transporters in plastids. Curr Opin Plant Biol **1:** 201–206

Flügge UI (1999) Phosphate translocators in plastids. Annu Rev Plant Physiol Plant Mol Biol **50:** 27–45

Flügge UI, Fischer K, Gross A, Sebald W, Lottspeich F, Eckerskorn C (1989) The triose phosphate-3-phosphoglycerate-phosphate translocator from spinach chloroplasts: nucleotide sequence of a full-length cDNA clone and import of the *in vitro* synthesized precursor protein into chloroplasts. EMBO J **8:** 39–46

Flügge UI, Freisl M, Heldt HW (1980) Balance between metabolite accumulation and transport in relation to photosynthesis by isolated spinach chloroplasts. Plant Physiol **65:** 574–577

Flügge UI, Heldt HW (1977) Specific labeling of a protein involved in phosphate transport of chloroplasts by pyridoxal-5-phosphate. FEBS Lett **82:** 29–33

Flügge UI, Heldt HW (1979) Phosphate translocator in chloroplasts: identification of the functional protein and characterization of its binding site. *In* E Quagliariello, F Palmieri, EM Klingenberg, eds, Function and Molecular Aspects of Biomembrane Transport. Elsevier/North Holland, Biomedical Press, Amsterdam, pp 373–382

Flügge UI, Stitt M, Freisl M, Heldt HW (1982) On the participation of phosporibulokinase in the light regulation of CO₂ fixation. Plant Physiol **69:** 263–267

Geiger DR, Servaites JC (1994) Diurnal regulation of photosynthetic carbon metabolism in C3 plants. Annu Rev Plant Physiol Plant Mol Biol **45:** 235–256

Gerhardt R, Stitt M, Heldt HW (1987) Subcellular metabolite levels in spinach leaves: regulation of sucrose synthesis during diurnal alterations in photosynthetic partition. Plant Physiol **83:** 399–407

Graeve K, von Schaewen A, Scheibe R (1994) Purification, characterization, and cDNA sequence of glucose-6-phosphate dehydrogenase from potato. Plant J **5:** 353–361

Hanke G, Bowsher CG, Jones MN, Tetlow I, Emes MJ (1999) Proteoliposomes and plant transport proteins. J Exp Bot **50:** 1715–1726

Hartwell J, Bowsher CG, Emes MJ (1996) Recycling of carbon in the oxidative pentose phosphate pathway in non-photosynthetic plastids. Planta **200:** 107–112

Heber U, Hallier UW, Hudson MA (1967) Untersuchungen zur intrazellulären Verteilung von Enzymen und Substraten in der Blattzelle: II. Lokalisation von Enzymen des reduktiven und des oxidativen Pentosephosphat-Zyklus in den Chloroplasten und permeabilität der Chloroplasten-membran gegenüber Metaboliten. Z Naturforsch **22:** 1200–1215

Heldt HW (1976) Transfer of substrates across the chloroplast envelope. Horizons Biochem Biophys **2:** 199–219

Heldt HW, Portis AR, Lilley RM, Mosbach A, Chon CJ (1980) Assay of nucleotides and other phosphate-containing compounds in isolated chloroplasts by ion exchange chromatography. Anal Biochem **101:** 278–287

Henkes S, Sonnewald U, Badur R, Flachmann R, Stitt M (2001) A small decrease of plastid transketolase activity in antisense tobacco transformants has dramatic effects on photosynthesis and phenylpropanoid metabolism. Plant Cell **13:** 535–551

Herrmann KM, Weaver LM (1999) The shikimate pathway. Annu Rev Plant Physiol Plant Mol Biol **50:** 473–503

Higgins DG, Bleasby AJ, Fuchs R (1992) CLUSTAL V: improved software for multiple sequence alignment. Comput Appl Biosci **8:** 189–191

Izawa S, Maeda K, Miki T, Mano J, Inoue Y, Kimura A (1998) Importance of glucose-6-phosphate dehydrogenase in the adaptive response to hydrogen peroxide in *Saccharomyces cerevisiae*. Biochem J **330:** 811 817

Jefferson RA, Kavanagh ZA, Bevan MW (1987) GUS fusions: beta-glucuronidase as a sensitive and versatile gene fusion marker in higher plants. EMBO J **6:** 3901–3907

Jensen RA (1985) Shikimate/arogenate pathway: link between carbohydrate metabolism and secondary metabolism. Physiol Plant **66:** 164–168

Kammerer B, Fischer K, Hilpert B, Schubert S, Gutensohn M, Weber A, Flügge UI (1998) Molecular characterization of a carbon transporter in plastids from heterotrophic tissues: the glucose 6-phosphate/phosphate antiporter. Plant Cell **10:** 105–117

Kasahara M, Hinkle P (1977) Reconstitution and purification of the D-glucose transporter from human erythrocytes. J Biol Chem **252:** 7384–7390

Kopriva S, Koprivova A, Süss KH (2000) Identification, cloning and properties of cytosolic ribulose-5-phosphate 3-epimerase from higher plants. J Biol Chem **275:** 1294–1299

Lilley RMC, Chon CJ, Mosbach A, Heldt HW (1977) The distribution of metabolites between spinach chloroplasts and medium during photosynthesis *in vitro*. Biochim Biophys Acta **460:** 259–272

Loddenkötter B, Kammerer B, Fischer K, Flügge UI (1993) Expression of the functional mature chloroplast triose phosphate translocator in yeast internal membranes and purification of the histidine-tagged protein by a single metal-affinity chromatography step. Proc Natl Acad Sci USA **90:** 2155–2159

Martin W, Henze K, Kellerman J, Flechner A, Schnarrenberger C (1996) Microsequencing and cDNA cloning of the Calvin cycle/OPPP enzyme ribose-S-phosphate isomerase (EC 5.3.1.6) from spinach chloroplasts. Plant Mol Biol **30:** 795–805

Neuhaus HE, Thom E, Möhlmann T, Steup M, Kampfenkel K (1997) Characterization of a novel ATP/ADP translocator located in the plastid envelope of *Arabidopsis thaliana*. Plant J **11:** 73–82

Noctor G, Foyer CH (1998) Ascorbate and glutathione: keeping active oxygen under control. Annu Rev Plant Physiol Plant Mol Biol **49:** 249–279

Nowitzki U, Wyrich R, Westhoff P, Henze K, Schnarrenberger C, Martin W (1995) Cloning of the amphibolic Calvin cycle/OPPP enzyme ribulose-5-phosphate 3-epimerase from spinach chloroplasts: functional and evolutionary aspects. Plant Mol Biol **29:** 1279–1291

Saitou N, Nei M (1987) The neighbour-joining method: A new method for reconstructing phylogenetic trees. Mol Biol Evol **4:** 406–425

Schnarrenberger C, Flechner A, Martin W (1995) Enzymatic evidence for a complete oxidative pentose phosphate pathway in chloroplasts and an incomplete pathway in the cytosol of spinach leaves. Plant Physiol **108:** 609–614

Schnarrenberger C, Oeser A, Tolbert NE (1973) Two isoenzymes each of glucose-6-P dehydrogenase and 6-Phosphogluconate dehydrogenase in spinach leaves. Arch Biochem Biophys **154:** 438–448

Stitt M, ap Rees T (1979) Capacities of pea chloroplasts to catalyze the oxidative pentose phosphate pathway and glycolysis. Phytochemistry **18:** 1905–1911

Stitt M, Wirtz W, Heldt HW (1980) Metabolite levels during induction in the chloroplast and extrachloroplast compartments of spinach protoplasts. Biochim Biophys Acta **593:** 85–102

Streatfield SJ, Weber A, Kinsman EA, Häusler RE, Li J, Post-Beittenmiller D, Kaiser WM, Pyke KA, Flügge UI, Chory J (1999) The phospho*enol*pyruvate/phosphate translocator is required for phenolic metabolism, palisade cell development and plastid-dependent nuclear gene expression. Plant Cell **11:** 1609–1621

Truernit E, Schmid J, Epple P, Illig J, Sauer N (1996) The sink-specific and stress-regulated Arabidopsis *STP4* gene: enhanced expression of a gene encoding a monosaccharide transporter by wounding, elicitors and pathogen challenge. Plant Cell **8:** 2169–2183

von Schaewen A, Langenkamper G, Graeve K, Wenderoth I, Scheibe R (1995) Molecular characterization of the plastidic glucose 6-phosphate dehydrogenase from potato in comparison to its cytosolic counterpart. Plant Physiol **109:** 1327–1335

Weber A, Menzlaff E, Arbinger B, Gutensohn M, Eckerskorn C, Flügge UI (1995) The 2-oxoglutarate/malate translocator of chloroplast envelope membranes: molecular cloning of a transporter protein containing a 12-helix motif and expression of the functional protein in yeast cells. Biochemistry **34:** 2621–2627

Weber A, Servaites JC, Geiger DR, Kofler H, Hille D, Gröner F, Hebbeker U, Flügge UI (2000) Identification, purification and molecular cloning of a plastidic glucose translocator. Plant Cell **12:** 787–801

Winter H, Robinson DG, Heldt HW (1994) Subcellular volumes and metabolite concentrations in spinach leaves. Planta **193:** 530–535